Northumbria
University
NEWCASTLE

Wearable optical fiber sensor based on a bend singlemode-multimode-singlemode fiber structure for respiration monitoring

Yi-Neng Pang,[1]Bin Liu*, Juan Liu, Sheng-Peng Wan, Tao Wu, Xing-Dao He, Jinhui Yuan*, Xian Zhou, Keping Long, Qiang Wu*

***Abstract*— Respiration rate (RR) is an important information related to human physiological health. A wearable optical fiber sensor for respiration monitoring based on a bend singlemode-multimode-singlemode (SMS) fiber structure, which is highly sensitive to bend, is firstly proposed and experimentally demonstrated. The sensor fastened by an elastic belt on the abdomen of a person will acquire the respiration signal when the person breaths, which will introduce front and back movement of the abdomen, and thus bend of SMS fiber structure. Short-time Fourier transform (STFT) method is employed for signal processing to extract characteristic information of both the time and frequency domain of the measured waveform, which provides accurate RR measurement. Six different SMS fiber sensors have been tested by six individuals and the experimental results demonstrated that the RR signals can be effectively monitored among different individuals, where an average Pearson Correlation Coefficient of 0.88 of the respiration signal has been achieved, which agrees very well with that of commercial belt respiration sensor. The proposed technique can provide a new wearable and portable solution for monitoring of respiratory with advantage of easy fabrication and robust to environment.**

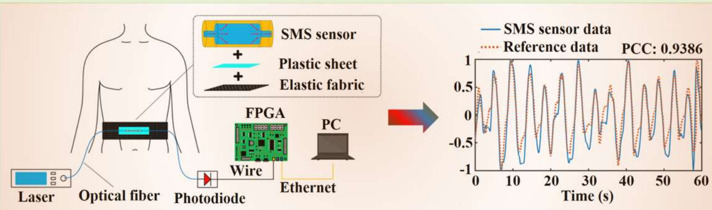

***Index Terms*— Optical fiber sensing, singlemode-multimode-singlemode (SMS) structure, Respiration monitoring, Pearson Correlation Coefficient**

I. Introduction

With the development of the modern medical technology, people pay more and more attention to physical health related parameters, such as respiration rate (RR) [1]. The human RR is normally detected by electronic sensor (typically piezoelectric sensor) and optical sensor [2-7]. Compared with the traditional piezoelectric sensor, the optical fiber sensor technique has many advantages such as the high sensitivity, resistence to corrosion and immunity to electromagnetic interference. There are mainly two types of optial fiber sensors by classifying demodulation methods: the intensity and the wavelength demodulated sensor [8]. In 2014, W. Zheng *et al.* designed an intensity-based notched polymer optical fiber fabric strain sensor for monitoring respiration [9]. In 2019, F. Z. Tan *et al.* proposed to use twin-core fiber based sensor to detect the human respiration and heartbeat signals [10]. In 2020, an in-line few-mode fiber Mach-Zehnder interferometer structure sensor is proposed by R. H. Wang *et al.* and applied to the respiration monitoring [11]. Fiber Bragg Grating (FBG) is also applied to monitor respiration, by utilizing its sensing property to strain, curvature, temperature, and relative humidity [12-15]. In 2020, Aizhan Issatayera *et al.* proposed a FBGs array-based system attached to the human chest and abdomen for respiration monitoring, which adopted multi-point measurements to counteract the interference of body measurements [16]. In 2019, Diaz *et al.* proposed a portable interrogator for dynamic assessment of knee angle and displacement by embedding FBG and FPI in different flexible structures [17]. In 2018, Bonefacino *et al.* proposed an ultra-fast polymer optical fibre Bragg grating inscription for human heartbeat and respiratory monitoring [18]. In addition to FBG, other wavelength demodulated sensors are utilized to acquire respiration signals. In 2019, K. Li *et al.* proposed a novel optical active fiber sensing technique based on the lasing wavelength demodulation for monitoring the human pulse and respiration

This work was jointly supported by National Natural Science Foundation of China (NSFC) (11864025, 61665007, 62065013); Natural Science Foundation of Jiangxi Province (Grant No. 20192ACB20031 and 20192ACBL21051); Major academic and technical leaders funding program of Jiangxi, China (Grant No. 20172BCB22012). (*Correspondence authors: Qiang Wu, Bin Liu and Jinhui Yuan*)

Yi-Neng Pang, Bin Liu, Juan Liu, Sheng-Peng Wan, Tao Wu, Xing-Dao He and Qiang Wu are with Key Laboratory of Nondestructive Test (Ministry of Education), Nanchang Hangkong University, Nanchang 330063, China (e-mail: fuyaohonghu@126.com; liubin@nchu.edu.cn; 18042@nchu.edu.cn; spwan@nchu.edu.cn; wutccnu@nchu.edu.cn; hxd@nchu.edu.cn; qiang.wu@northumbria.ac.uk). Qiang Wu is also with Faculty of Engineering and Environment, Northumbria University, Newcastle Upon Tyne NE1 8ST, UK

Jinhui Yuan, Xian Zhou and Keping Long are with the Research Center for Convergence Networks and Ubiquitous Services, University of Science & Technology Beijing, Beijing 100083, China. (e-mail: yuanjinhui81@163.com; zhouxian219@foxmail.com; longkeping@ustb.edu.cn).

[19]. There are other types of optical fiber sensor applied to detect the respiratory signals. For example, Leal-Junior *et al.* proposed a polymer optical fiber-based sensor for simultaneous measurement of breath and heartbeat rate under dynamic movements [20-21]. Such as the optical interferometric sensor, the fiber-optic fluorescence sensor, the plastic optical fiber sensor, the optical fiber micro bend sensor, etc. [22-26]. However, these sensors mentioned above have disadvantages of either with complex structure, or relatively low sensitivity, etc.

Recently we proposed to use a bend SMS fiber structure for respiration monitoring [27]. In this application, the bend SMS fiber structure is attached to a respiration mask, where the breath will introduce air blow to the SMS fiber sensors, resulting in the change of bend radius. This sensor design isn't wearable/robust due to the use of respiration mask, which isn't comfortable for people wearing it. In this work, a wearable and compact optical fiber sensor based on a bend SMS fiber structure for respiration monitoring is proposed by attaching the SMS fiber sensor on an elastic belt, which is fastened on the abdomen of a person. Dynamic short-time Fourier transform (STFT) signal processing method, which can extract characteristic information of both the time and frequency domain of the signal is employed to achieve very accurate measurement. The measured results were compared with that of a commercial belt respiration sensor.

II. Theoretical Analysis and Simulation

A. SMS fiber structure sensing principle

The SMS fiber structure is configured by fusion splicing a short section of multimode fiber (MMF) between two singlemode fibers (SMFs), as shown in Fig. 1(a). Both fundamental and high-order eigen modes of the MMF will be excited when light transmits from input SMF to MMF. These modes will propagate independently in the MMF section and interference at the output SMF, which can be acquired by an optical spectrum analyzer (OSA).

For a straight MMF, the refractive index (RI) is symmetrically distributed along the fiber axis. However, when the MMF is curved, the RI distribution is radius dependent and an equivalent RI distribution is defined as follows [27-29]:

$$n = n_0(1 + \frac{x}{R_{eff}}) \quad (1)$$

where $n_0(x, y)$ is the RI of the straight fiber and R_{eff} is the equiralent bend radius which can be expressed as follows:

$$R_{eff} = \frac{R}{1-(n_0^2/2)[P_{12}-v(P_{11}+P_{12})]} \quad (2)$$

where R is the bend radius of the fiber, v is the Poisson ratio and P_{11} and P_{12} are components of the photoelastic tensor.

Based on the above theoretical analyses, numerical simulations have been conducted employing the beam propagation method (BPM) with a 2D model. The simulation conditions were based on a mesh size in the X and Z directions of 0.1 μm and 1 μm, respectively, and the boundary condition adopted a perfectly matched layer (PML) condition in the model. The SMF has a core and cladding diameter of 8 μm and 125 μm respectively. The core diameter and cladding diameter of MMF are set to 105 μm and 125 μm respectively. The length of the MMF fiber is 30 mm. The core and cladding RI of both MMF and SMF are 1.4497 and 1.4418 respectively. The simulated transmission spectrum of a straight SMS fiber structure is shown in the Fig. 1(b).

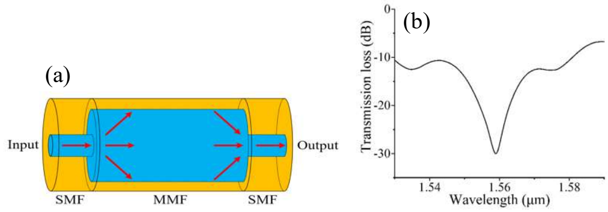

Fig. 1 (a) A schematic diagram of an SMS optical fiber sensor, (b) simulated transmission power of the SMS optical fiber sensor.

B. SMS fiber sensor curvature experiment

The experimental setup of using an SMS fiber structure for curvature measurement is shown in Fig. 2. The input SMF is connected to an amplified spontaneous emission (ASE) broadband light source and the output SMF is connected to an OSA (Yokogawa AQ6370D) to measure the transmission spectrum of the sensor. Both ends of the SMS fiber sensor are fixed to a translation stage which can be used to adjust the curvature of the sensor by moving forward/backward the translation stage as shown in Fig. 2. In our experiments, three different MMF lengths of 20 mm, 30 mm and 40 mm were used to study the influence of MMF length on the performance of the bend SMS fiber sensor. In the experiment, the step increment of translation stage is 5 μm. The curvature of the SMS fiber sensor can be calculated by adopting the approximation of the sine function to the second-order as [30]:

$$C = 2\frac{sin(L_0C/2)}{L_0-\Delta y} \approx \sqrt{\frac{24\Delta y}{L_0^3}} \quad (3)$$

where L_0 is the initial distance between two translation stages, Δy is the displacement applied by the translation stage.

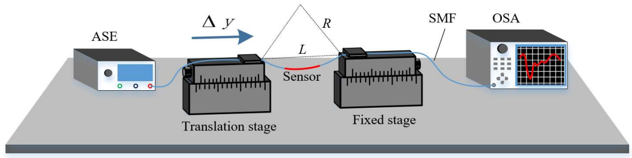

Fig.2. Schematic diagram of the experimental setup for SMS structure optical fiber sensor curvature experiment.

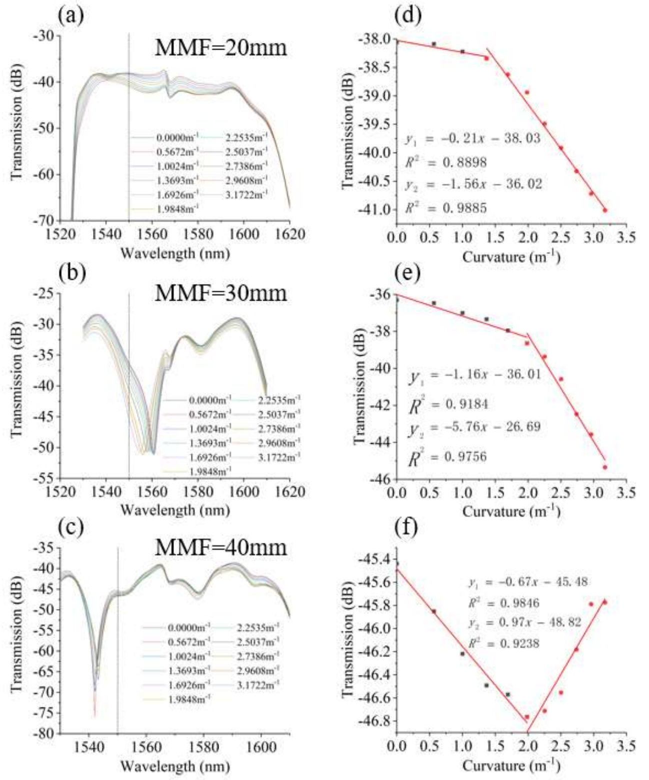

Fig.3. Transmission spectrum in response to different curvatures of the sensor with (a) 20 mm MMF, (b) 30 mm MMF and (c) 40 mm MMF. (d) Linear fit of the power variation at wavelength 1550 nm for SMS sensor with (d) 20 mm MMF, (e) 30 mm MMF and (f) 40 mm MMF.

The power variation at 1550 nm wavelength is extracted from the spectra with different curvature value, because the 1550 nm light laser source will be used in further experiments of respiration monitoring. Figures 3(a-c) shows the transmission spectra of the sensors with three different MMF length under different curvatures and Figures 3(d-f) shows the extracted power variations at wavelength 1550 nm, where two sets of linear fits were applied to that of each SMS fiber sensor. As shown in Fig. 3(d-f), for each SMS fiber sensor, the sensitivity to bend is different. For example, the SMS sensor with 30 mm MMF length has the highest sensitivity and the best linearity among the three optical sensors with different MMF length when the curvature ranges from 0 m^{-1} to 3.1722 m^{-1} so that we choose the SMS sensor with 30 mm as respiration sensor in the following experiment.

III. Respiration Monitoring System Architecture

Figure 4(a) shows a schematic diagram of the respiration monitoring system, which composed of five components, including a CW (Continuous Wave) laser (1550 nm) in the Figure 4(b), an elastic belt embedded with the SMS fiber sensor, a photodiode in the Figure 4(c), a FPGA (Field Programmable Gate Array) voltage acquisition unit and a PC (Personal Computer). Figure 4(d) shows a picture of the elastic belt, which consists of an SMS fiber sensor, a piece of plastic sheet and an elastic fabric. The output light intensity is detected by an InGaAs photodiode (PDA10CS-EC, THORLABS), which transferred optical signal to electrical signal and transmitted to an FPGA. The sampling rate of the FPGA voltage acquisition component is 50 Hz, which is controlled by a PC. Figure 4(e) shows a picture of the wearable sensor fastened on the abdomen of a person under RR test. It is noted that due to the small size of optical source and sensor demodulation system, the respiration monitoring system is portable, which can be used in hospitals for patients' RR monitoring. In the future investigation, a smart phone will be used to replace laptop to acquire and process respiration signals, which enables the whole system wearable.

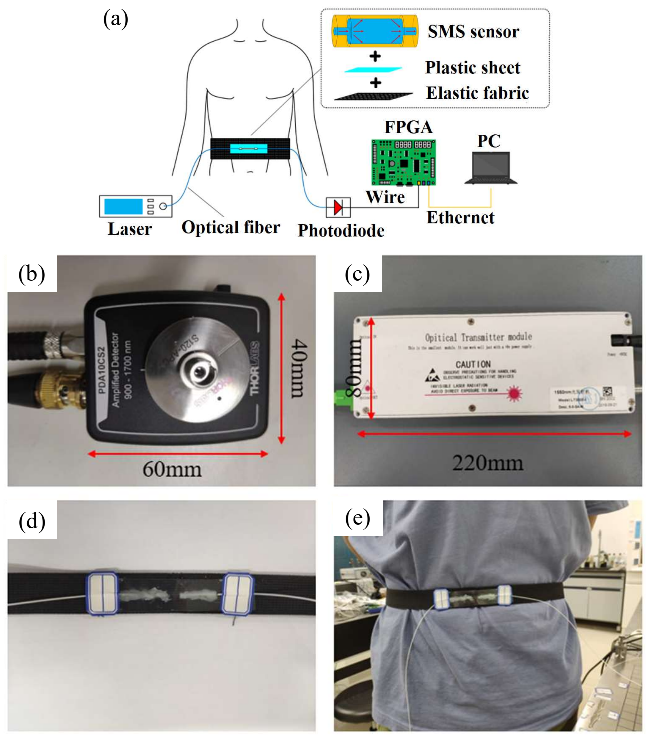

Fig.4. Experiment setups. (a) system architecture, (b) photodiode, (c) laser source, (d) the elastic belt structure and (e) wear method.

IV. Experimental Results and Discussion

A. Respiration signal preprocessing

Figure 5(a) shows measured power (voltage) variations within 60 seconds' periodic respiration, where periodic signal with a baseline drift can be observed . Figure 5(b) gives Fast Fourier Transform (FFT) of the respiration signal. The baseline drift and interference [shown in Figs. 5(a) and (b)] will have influence on the subsequent accuracy analysis result of respiration monitoring. Wavelet decomposition method is thus used to eliminate the baseline drift and interference due to its decorrelation and flexibility in signal processing field. $L^2(R)$ represents the square integrable real number space, i.e. limited energy signal space, R is a real number. Assumed that $g(t) \in L^2(R)$, t is the time, $\psi(t)$ is a wavelet generating function. Then the continous wavelet transform is [31]:

$$W_g(a,b) = |a|^{-1/2} \int_R g(t)\psi * (\frac{t-b}{a})dt \quad (4)$$

where a and b are the scaling and translation factor, respectively. Continuous wavelet discretization is used in the application:

$$a = a_0^j, b = ka_0^j b_0 \quad (5)$$

where k and j are integers, a_0 is the fixed scaling step length and b_0 is the fixed translation step length. Then the coefficient of the discretize wavelet transform:

$$W_{g,k}(t) = a_0^{-j/2}\int_R \psi * \left(a_0^{-j/2}t - kb_0\right)dt \qquad (6)$$

The wavelet reconstruction formula is:

$$g(t) = Q\sum_{-\infty}^{\infty}\sum_{-\infty}^{\infty} W_{j,k}\, a_0^{-j/2}\psi(a_0^{j}t - kb_0) \qquad (7)$$

where Q is an independent constant of the signal. The raw signal is decomposed by wavelet transform ie. Eq (6) to obtain the detaile coefficients of the high frequency and approximation coefficient of the low frequency. Since the baseline drift and interference exists in the low frequency, we remove the approximation coefficient of the low frequency and keep detail coefficients of high frequency only. The signal is thus processed as shown in the Figs. 5(c) and (d) by the wavelet reconstruction ie. Eq (7). At the same time, noise interference exists in respiration signal in Figs. 5(c) and (d). We also adopt wavelet decomposition to denoise the respiration signal by removing the detail coefficients of the high frequency because noise exists in the high frequency. Most of the noise of the respiration signal is thus filtered using the above siganl processing method [shown in Figs. 5(e) and (f)].

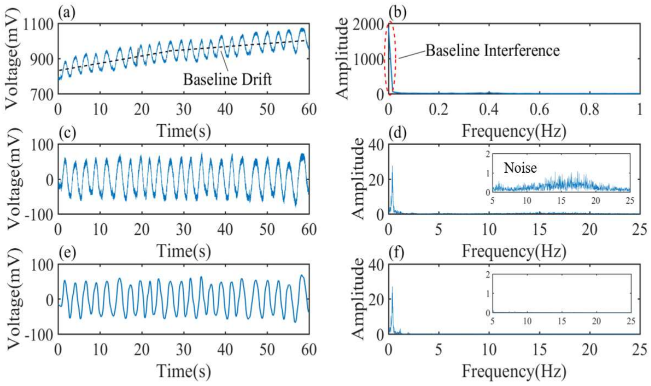

Fig.5. Respiration signal preprocessing analysis. (a) The time domain and (b) the frequency domain of raw signal; (c) the time domain and (d) the frequency domain of removed baseline interference signal; (e) the time domain and (f) the frequency domain of denoised signal.

B. RR monitoring

A female and a male volunteer participate the experimental study of the RR monitoring. The signal preprocessed by the wavelet decomposition method is shown in Figs. 6(a) and (c), and the FFT method is applied to both Figs. 6(a) and (c) to extract the frequency information as shown in Figs. 6(b) and (d). The results of respiration monitoring indicate that the RR of the female and male volunteer are 0.35 Hz and 0.25 Hz respectively, indicating that the female volunteer has higher RR than that of the male volunteer. The experimental result indicates that the proposed SMS fiber sensor can measure RR accurately.

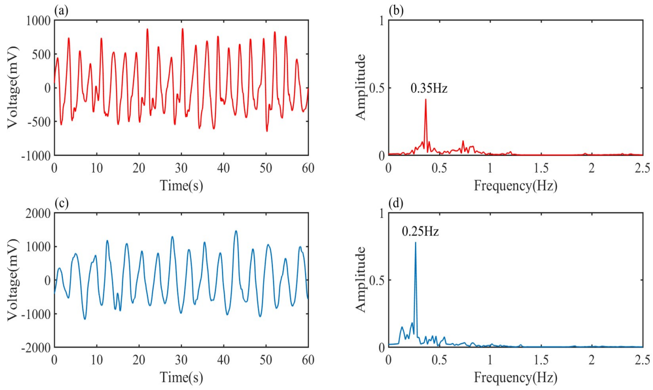

Fig.6. RR of different individual analysis. Measured time domain of the RR by (a) the female and (c) male volunteer; extracted normalized frequency spectrum of the RR by (b) the female and (d) male volunteer.

The classic FFT can be used to analyze the regular signal. However, the respiration signal is sometimes not a regular signal (for example, RR varies) caused by the change of human physiological condition. In this case, the classic FFT cannot be used to analyze the signal and thus the STFT method is used to process the signal, because the result calculated by STFT has the characteristics of both the time and frequency domain of the signal. The signal $x(t)$ transformed By STFT can be defined as [32]:

$$F_{STFTx}(t,f) = \int_{-\infty}^{\infty} x(u)h(u-t)e^{-j2\pi fu}du \qquad (8)$$

where f represents the frequency, $h(t)$ is a window function at u on the time axis. Figures 7(a) and (b) recorded the waveform of respiration apnea and recovery, and respiration variation after exercise, respectively. The corresponding instantaneous frequency after STFT are shown in Figs. 7(c) and (d). It can be observed in Fig. 7(c) that the respiration frequency value is 0.3 Hz in time range 0-27 s; the respiration apnea happens in 27-45 s and recovery in 45-60 s which corresponds to the waveform in the Fig. 7(a). Figure 7(d) indicates the instantaneous frequency variation ranges from 1.67 Hz to 0.4 Hz after exercise. The above experimental results confirm that STFT is an effective method for data processing of the measurement of the RR variation.

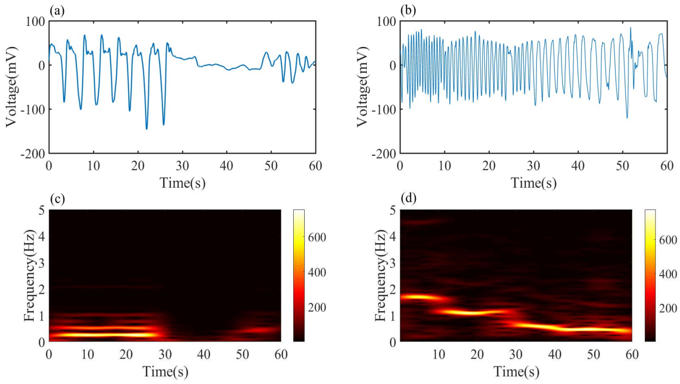

Fig.7. Irregular respiration signal analysis. (a) the time domain and (c) the frequency domain of respiration apnea and recovery; (b) the time domain and (d) the frequency domain of respiration after exercise.

C. Accuracy analysis of respiration monitoring

In order to verify the accuracy of respiration monitoring with the SMS structure optical fiber sensor, a commercial belt respiration sensor (HKH-11C, Hefei Huake Information Technology Co.Ltd) was selected as a reference for the synchronous measurement of RR.

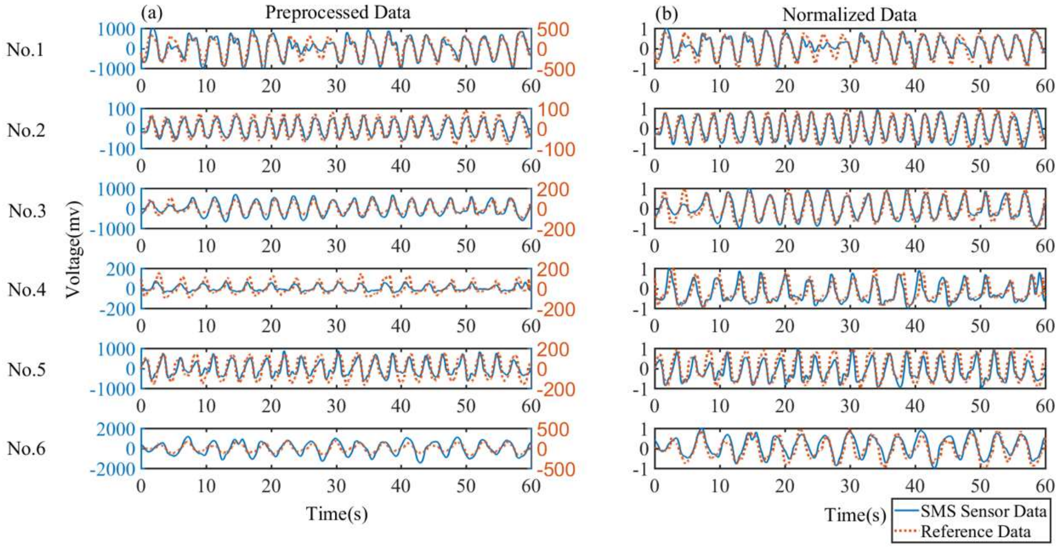

Fig.8. Comparation between respiration data of the SMS structure optical fiber sensor and the commercial belt respiration sensor. (a) Raw data after preprocessing. (b) Normalized data.

Six volunteers participate the comparison of respiration monitoring. In the experiments, both the commercial belt respiration sensor and the SMS sensor were tied to the abdomen of the volunteers for respiration monitoring. The sample frequency of both systems is 50 Hz and the measurements were carried out simultaneously. Figure 8(a) shows the measured respiration waveforms for the six volunteers, where blue and orange waveforms correspond to the preprocessed data of the SMS sensor and the commercial belt respiration sensor in 60 seconds respectively. Since the collected voltages between the two sensor systems are different, a normalization of these data is applied, and the result is shown in Fig. 8(b).

Table.1. Result of the signals from the SMS fiber sensor correlated to the signals from the commercial belt respiration sensor.

Volunteer	Sample size (number of data collected)	PCC
1	3000	0.9214
2	3000	0.8972
3	3000	0.9220
4	3000	0.8168
5	3000	0.8681
6	3000	0.8986

To reveal the relationship between the results measured by both SMS fiber sensor and commercial respiration sensor, Pearson Correlation Coefficient (PCC) is introduced to calculate the degree of linear correlation between these measurements, which is defined by [11]:

$$p = \frac{N\sum x_i y_j - \sum x_i \sum y_j}{\sqrt{N\sum x_i^2 - (\sum x_i)^2}\sqrt{N\sum y_i^2 - (\sum y_i)^2}} \tag{9}$$

where x_i and y_i are the sample values of the two groups of data obtained from the SMS sensor and the commercial sensor, respectively. N is the sample size of the data. In a general way, the PCC exceeded 0.8 indicates a strong correlation between the two groups of data [33]. The PCCs of the above measured results of six volunteers are summarized in Table 1. As can be seen in Table 1, the PCCs of all 6 groups' data are higher than 0.8, and the best PCC is as high as 0.922. The above results demonstrated that the proposed sensor has a strong correlation with standard respiration monitoring device and can be used for accurate human respiratory monitoring.

To study the long-term stability of the SMS sensor for respiration monitoring, a volunteer participates measurements for the long-term verification. The sensor with lowest PCC was selected for the long-term stability test. Fig.9 shows the raw data after preprocessing and the normalized data of the first and the second measurements, where there is a gap of two weeks between the tests using the same SMS and reference sensor. The PCC of the first measurement is 0.9337 and the PCC of the second measurement in two weeks is 0.9386. The results of the measurement are higher than 0.8, which indicates that the SMS sensor is effective for long-term respiration monitoring.

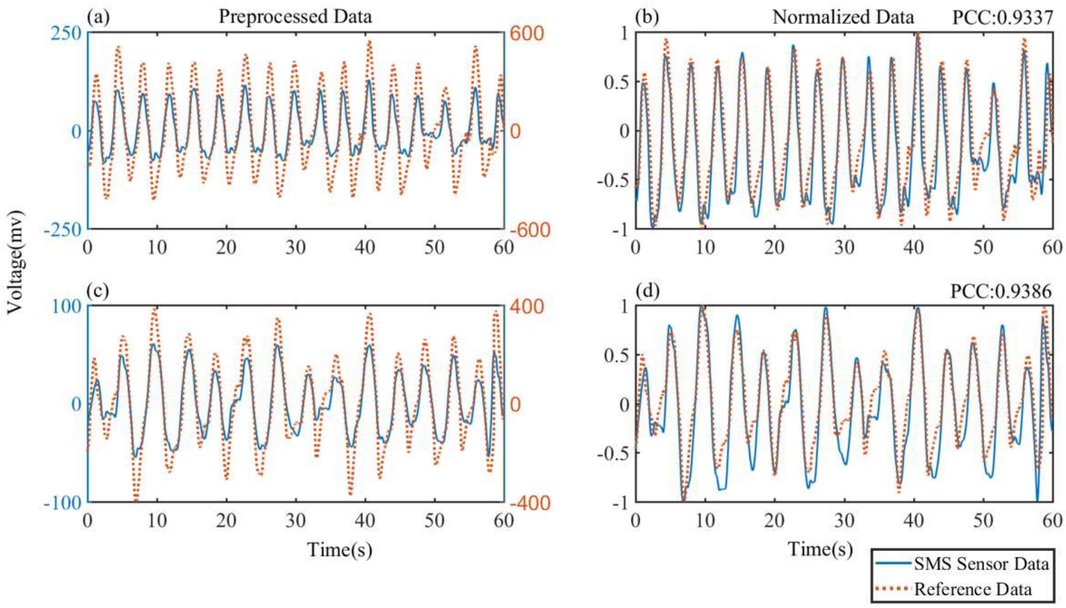

Fig.9.The long-term validity verification of the SMS sensor for respiration monitoring. (a) The raw data after preprocessing and (b) the normalized data in the first measurement; (c) The raw data after preprocessing and (d) the normalized data in the second measurement.

V. Conclusion

In conclusion, a wearable respiration monitoring setup based on a SMS structure optical fiber sensor was proposed and experimentally demonstrated, which can be used to monitor both regular and irregular RR caused by different human physiological conditions. The SMS sensor embedded elastic belt structure, which is fastened on the abdomen position, can acquire the respiration signal because of the undulating movement of the abdomen. Both the regular and irregular RR can be achieved by wavelet decomposition, FFT and STFT methods. Accuracy experiments of the optical fiber sensor for respiration monitoring is carried out by comparing with a commercial belt respiration sensor in the sample group of six volunteers, where a correlation indicator PCC is calculated. The experimental results indicate that the PCCs of all volunteers exceed 0.8 (strong correlation). Long-term stability of the SMS sensor was also studied by measuring two sets of respiration signals of the same volunteer, where two weeks gap was applied to the two measurements. The result shows that the SMS sensor has good long-term stability. The respiration monitoring technique based on the proposed SMS sensor may play an important role in the human health monitoring application. It is noted that temperature will have impact on the wavelength response of the sensor and compensation technique has been proposed by Arnaldo *et al*. [34]. However, in our RR measurement, since the frequency of RR is much higher than that of temperature variation, the impact of temperature can be ignored. Body movement also has negative impact on the measurement accuracy. A possible solution is to integrate multiple SMS fiber sensors into the elastic belts and attach to different positions of the body. Using diversity-based signal processing method [16] to process the measurements with different SMS sensors, it is possible to compensate the influence of body movements and realize accurate RR monitoring. Measurement of other physiological parameters are also possible using the developed SMS sensor. For example, human pulse and heartbeat rate can be measured by attaching the SMS sensor to the brachial artery and chest of a person.

References

[1] E. Fleming, C. Voscopoulos, and E. George, "Non-invasive respiratory volume monitoring identifies opioid-induced respiratory depression in an orthopedic surgery patient with diagnosed obstructive sleep apnea: a case report," *Journal of Medical Case Reports*, vol. 9, no. 1, Apr. 2015.

[2] S. Atalay, S. Erdemoglu, V. S. Kolat, T. Izgi, E. Akgeyik, H. C. Yilmaz, H. Kaya, and F. E. Atalay, "A rapid response humidity sensor for monitoring human respiration with TiO_2 -Based nanotubes as a sensing layer," *Journal of Electronic Materials,* vol. 49, no. 5, pp. 3209-3215, Feb. 2020.

[3] A. Rasheed, E. Iranmanesh, W. W. Li, Y. B. Xu, Q. Zhou, H. Ou, and K. Wang, "An active self-driven piezoelectric sensor enabling real-time respiration monitoring," *Sensors*, vol. 19, no. 14, pp. 3214, Jul. 2019.

[4] F. Sandberg, M. Holmer, and B. Olde, "Monitoring respiration using the pressure sensors in the dialysis machine," *Physiological Measurement,* vol. 40, no. 2, pp. 25001, Feb. 2019.

[5] Y. Pang, J. Jian, T. Tu, Z. Yang, J. Ling, Y. X. Li, X. F. Wang, Y. C. Qiao, H. Tian, Y. Yang, and T. L. Ren, "Wearable humidity sensor based on porous graphene network for respiration monitoring," *Biosensors and Bioelectronics*, vol. 116, pp. 123-129, Sep. 2018.

[6] Z. Liu, S. Zhang, Y. M. Jin, H. Ouyang, Y. Zou, X. X. Wang, L. X. Xie, and Z. Li, "Flexible piezoelectric nanogenerator in wearable self-powered active sensor for respiration and healthcare monitoring," *Semiconductor Science and Technology*, vol. 32, no. 6, pp. 1, May. 2017.

[7] Y. P. Su, C. P. Li, M. J. Li, H. J. Li, S. Xu, L. R. Qian, and B. H. Yang, "Surface acoustic wave humidity sensor based on three-dimensional architecture graphene/PVA/SiO_2 and its application for respiration monitoring," *Sensors and Actuators B: Chemical*, vol. 308, Jan. 2020.

[8] M. A. Zawawi, S. O'Keffe, and E. Lewis, "Intensity-modulated fiber optic sensor for health monitoring applications: a comparative review," *Sensor Review*, vol. 33, no. 1, pp. 57-67, 2013.

[9] W. Zheng, X. M. Tao, B. Zhu, G. F. Wang, and C. Y. Hui, "Fabrication and evaluation of a notched polymer optical fiber fabric strain sensor and its application in human respiration monitoring," *Textile Research Journal*, vol. 84, no. 17, pp. 1791-1802, Sep. 2014.

[10] F. Z. Tan, S. Y. Chen, W. M. Lyu, Z. Y. Liu, C. Y. Yu, C. Lu, and H. Y. Tam, "Non-invasive human vital signs monitoring based on twin-core optical fiber sensors," *Biomedical Optics Express*, vol. 10, no. 11, pp. 5940-5951, Nov. 2019.

[11] R. H. Wang, J. Zhao, Y. Sun, H. Yu, N. Zhou, H. X. Zhang, and D. G. Jia, "Wearable respiration monitoring using an in-line few-mode fiber Mach-Zehnder interferometric sensor," *Biomedical Optics Express*, vol. 11, no. 1, pp. 316-329, Jan. 2020.

[12] M. Fajkus, J. Nedoma, R. Martinek, J. Brablik, J. Vanus, M. Novak, S. Zabka, V. Vasinek, P. Hanzlikova, and L. Vojtisek, "MR fully compatible and safe FBG breathing sensor: a practical solution for respiratory triggering," *IEEE Access*, vol. 7, pp. 123013-123025, Aug. 2019.

[13] L. Dziuda, F. W. Skibniewski, M. Krej, and P. M. Baran, "Fiber Bragg grating-based sensor for monitoring respiration and heart activity during magnetic resonance imaging examinations," *Journal of Biomedical Optics*, vol. 18, no. 5, pp. 057006, May. 2013.

[14] J. H. Wo, H. Wang, Q. Z. Sun, P. P. Shum, and D. Liu, "Noninvasive respiration movement sensor based on distributed Bragg reflector fiber laser with beat frequency interrogation," *Journal of Biomedical Optics*, vol. 19, no. 1, pp. 17003, Jan. 2014.

[15] C. Massaroni, M. Zaltieri, D. Lo Presti, A. Nicolò, D. Tosi, and E. Schena, "Fiber Bragg Grating sensors for cardiorespiratory monitoring: A Review," *IEEE Sensors Journal*, 2020.

[16] A. Issatayeva,, A. Beisenova, D. Tosi, and C. Molardi," Fiber-Optic Based Smart Textiles for Real-Time Monitoring of Breathing Rate," *Sensors,* vol. 20, no. 12, pp. 3408, Jun. 2020.

[17] A. R. D. Camilo, A. G. Leal-Junior, M. A. Letícia, F. C. A. Paulo, J. P. Maria, A. M. Carlos, A. Frizera, and R. N. R. Moisés, "Perrogator: A Portable Energy-Efficient Interrogator for Dynamic Monitoring of Wavelength-Based Sensors in Wearable Applications," *Sensors,* vol. 19, no. 13, pp. 2962, Jul. 2019.

[18] J. Bonefacino, H. Tam, T. S. Glen, X. Cheng, C. J. Pun, J. Wang, P. Lee, M. V. Tse, and S. T. Boles, "Ultra-fast polymer optical fibre Bragg grating inscription for medical devices," *Light: Science & Application*, vol. 7, no. 3, pp. 17161, Mar. 2018.

[19] K. Li, L. Xia, H. Yi, S. Y. Li, Y. Wu, and Y. M. Song, "Optical active fiber sensing technique based on the lasing wavelength demodulation for monitoring the human respiration and pulse," *Sensor and Actuators A: Physical*, vol. 296, pp. 45-51, Jul. 2019.

[20] A. G. Leal-Junior, C. R. C. R. Díaz, C. Leitão, M. J. M. J. Pontes, C. Marques, and A. Frizera, "Polymer optical fiber-based sensor for simultaneous measurement of breath and heart rate under dynamic movements," *Optics and Laser Technology*, vol. 109, pp. 429–436, Aug. 2018.

[21] A. Leal-Junior, A. Frizera, M. J. Pontes, A. Fasano, G. Woyessa, O. Bang, and C. A. F. Marques, "Dynamic mechanical characterization with respect to temperature, humidity, frequency and strain in mPOFs made of different materials," *Optical Materials Express*, vol. 8, no. 4, pp. 804-815, Apr. 2018.

[22] S. Sprager, and D. Zazula, "Heartbeat and espiration detection from optical interferometric signals by using a multimethod approach," *IEEE Transactions on Biomedical Engineering*, vol. 57, no. 10, pp. 2633-2639, Oct. 2012.

[23] R. S. Chen, F. Formenti, A. Obeid, C. E. W. Hahn, and A, D. Farmery, "A fibre-optic oxygen sensor for monitoring human breathing," *Physiological Measurement*, vol. 34, no. 9, pp. 71-81, Aug. 2013.

[24] D. Sartiano, and S. Sales, "Low cost plastic optical fiber pressure sensor embedded in mattress for vital signal monitoring," *Sensors*, vol. 17, no. 12, Dec. 2017.

[25] H. F. Hu, S. J. Sun, R. Q. Lv, and Y. Zhao, "Design and experiment of an optical fiber micro bend sensor for respiration monitoring," *Sensors and Actuators A: Physical*, vol. 251, pp. 126-133, Oct. 2016.

[26] S. Sprager, and D. Zazula, "Detection of heartbeat and respiration from optical interferometric signal by using wavelet transform," *Computer Methods and Programs in Biomedicine*, vol. 111, no. 1, pp. 41-51, Mar. 2013.

[27] X. Li, D. Liu, R. Kumar, W. P. Ng, Y. Q. Fu, J. Yuan, C. Yu, Y. Wu, G. Zhou, G. Farrell, Y. Semenova, and Q. Wu, "A simple optical fiber interferometer based breathing sensor", *Measurement Science and Technology*, vol. 28, no. 3, 2017

[28] Q. Wu, M. Yang, J. Yuan, H. P. Chan, Y. Ma, Y. Semenova, P. Wang, C. Yu, and G. Farrell, "The use of a bend singlemode-multimode-singlemode (SMS) fiber structure for vibration sensing", *Optics and Laser Technology*, vol. 63, pp. 29-33, 2014

[29] Q. Wu, Y. Semenova, P. Wang, A. M. Hatta, and G. Farrell, "Experimental demonstration of a simple displacement sensor based on a bent single-mode–multimode–single-mode fiber structure", *Measurement Science and Technology*, 22 025203 (2011)

[30] M. Xiong, H. Gong, Z. Wang, C. L. Zhao, and X. Dong, "Fiber curvature sensor based on spherical-shape structures and long-period grating," *Optics and Lasers in Engineering*, vol. 86, pp. 356-359, Jul. 2016.

[31] X. B. Fan, B. Zhao, and B. X. Fan, "Wavelet decomposition and nonlinear prediction of nonstationary vibration signals," *Noise & Vibration Worldwide*, vol. 51, no. 3, pp. 52-59. 2020.

[32] H. Zhivomirov, "On the development of STFT-analysis and ISTFT-synthesis routines and their practical implementation," *TEM Journal*, vol. 8, no. 1, pp. 56-64, Feb. 2019.

[33] Y. Q. Liu, Y. Mu, K. Y. Chen, Y. M. Li, and J. H. Guo, "Daily activity feature selection in smart homes based on Pearson Correlation Coefficient," *Neural Processing Letters*, vol. 51, no. 2, pp. 1771-1787, 2020.

[34] A. Leal-Junior, A. Frizera, C. Díaz, C. Marques, M. Ribeiro, and M. J. Pontes, "Material features based compensation technique for the temperature effects in a polymer diaphragm-based FBG pressure sensor," *Optics Express*, vol. 26, no. 16, pp. 20590-20602, Aug. 2018.

Yi-Neng Pang received the B.S. degree from Hunan Institute of Engineering in 2017. He is currently pursuing the M.S. degree in optical engineering with Nanchang Hangkong University. His current research interests include optical fiber sensing and signal processing.

Bin Liu received his B.S. and Ph.D. degree from Sun Yat-sen University, China. Dr. Liu is an associate Professor with Key Laboratory of Nondestructive Test (Ministry of Education) of Nanchang Hangkong University, China. His main research interest is fiber optic sensing.

Juan Liu received her Ph.D. degree from Beijing Normal University, China. She is a lecture with Key Laboratory of Nondestructive Test (Ministry of Education) of Nanchang Hangkong University, China. Her main research interest is fiber optic sensing.

Sheng-Peng Wan received the B.S. and Ph.D. degrees from University of Electronic and Technology of China. He is a professor with Key Laboratory of Nondestructive Test (Ministry of Education) of Nanchang Hangkong University, China. His main research interest is fiber optic sensing.

Tao Wu received his Ph.D. degree in Optics from University of the Littoral Opal Coast and Anhui Institute of Optics and Fine Mechanics, China. In 2010, Dr. Wu joined Key Laboratory of Nondestructive Test (Ministry of Education) of Nanchang Hangkong University, China. His main research interest has been the development of high-sensitivity laser spectrometer for laboratory and field studies of atmospheric trace gases and aerosols.

Xing-Dao He was born in Jingan, China, in 1963. He received the Ph.D. degree in optics from Beijing Normal University, Beijing, China, in 2005. He is currently a Professor with the Key Laboratory of Nondestructive Test (Ministry of Education), Nanchang Hangkong University, China. His current research interests include light scattering spectroscopy, optical holography, and information processing.

Jinhui Yuan received the Ph.D. degree in physical electronics from Beijing University of Posts and Telecommunications (BUPT), Beijing, China, in 2011. He is currently a Professor at the Department of computer and communication engineering, University of Science and Technology Beijing (USTB). He was selected as a Hong Kong Scholar at the Photonics Research Centre, Department of Electronic and Information Engineering, The Hong Kong Polytechnic University, in 2013. His current research interests include photonic crystal fibers, silicon waveguide, and optical fiber devices. He is the Senior Members of the IEEE and OSA. He has published over 200 papers in the academic journals and conferences.

Xian Zhou received the Ph.D. degree in electromagnetic field and microwave technology from Beijing University of Posts and Telecommunications (BUPT), Beijing, China, in 2011. She is currently a Professor at the Department of computer and communication engineering, University of Science and Technology Beijing (USTB). She was selected as a Hong Kong Scholar at the Photonics Research Centre, Department of Electronic and Information Engineering, The Hong Kong Polytechnic University, in 2013. Her research interests are focused on high-speed optical communications, short reach communications, and digital signal processing. She has published over 150 papers in the academic journals and conferences.

Keping Long (SM'06) received the M.S. and Ph.D. degrees from the University of Electronic Science and Technology of China, Chengdu, China, in 1995 and 1998, respectively. From September 1998 to August 2000, he was a Postdoctoral Research Fellow with the National Laboratory of Switching Technology and Telecommunication Networks, Beijing University of Posts and Telecommunications (BUPT), Beijing, China. From September 2000 to June 2001, he was an Associate Professor with BUPT. From July 2001 to November 2002, he was a Research Fellow with the ARC Special Research Centre for Ultra Broadband Information Networks, University of Melbourne, Melbourne, Australia. He is currently a Professor and Dean with the School of Computer and Communication Engineering, University of Science and Technology Beijing. He has authored more than 200 papers and has delivered 20 keynote speeches. He is a Member of the Editorial Committee of Sciences in China Series F and China Communications. His research interests are optical internet technology, new-generation network technology, wireless information networks, value-added service, and secure technology of networks. Dr. Long has been a Technical Program Committee (TPC) and International Steering Committee member for COIN2003/04/05/06/07/08/09/10, IEEE IWCN2010, ICON04/06, and APOC2004/06/08; a Co-chair of the organization membership for the 2006 International Wireless Communications and Mobile Computing Conference; the TPC chair of COIN2005/2008; and a TPC Cochair of COIN2008/2010. He has been invited to talk at both international and local conferences. He received the National Science Fund for Distinguished Young Scholars of China in 2007 and was selected as the Chang Jiang Scholars Program Professor of China in 2008.

Qiang Wu received the B.S. and Ph.D. degrees from Beijing Normal University and Beijing University of Posts and Telecommunications, Beijing, China, in 1996 and 2004, respectively. From 2004 to 2006, he worked as a Senior Research Associate in City University of Hong Kong. From 2006 to 2008, he took up a research associate post in Heriot-Watt University, Edinburgh, U.K. From 2008 to 2014, he worked as a Stokes Lecturer at Photonics Research Centre, Dublin Institute of Technology, Ireland. He is with Faculty of Engineering and Environment, Northumbria University, Newcastle Upon Tyne, United Kingdom; Key Laboratory of Nondestructive Test (Ministry of Education), Nanchang Hangkong University, Nanchang 330063, China. His research interests include optical fiber interferometers for novel fiber optical couplers and sensors, nanofiber, microsphere sensors for bio-chemical sensing, the design and fabrication of fiber Bragg grating devices and their applications for sensing, nonlinear fibre optics, surface plasmon resonant and surface acoustic wave sensors. He has over 200 journal publications in the area of photonics and holds 3 invention patents. He is an Editorial Board Member of Scientific Reports, an Associate Editor for IEEE Sensors Journal and an Academic Editor for Journal of Sensors.